Cellular and Molecular Biology

Journal homepage: www.cellmolbiol.org

Papaverine Infusion Through Aortic Root before Cardiac Self-recovery in Heart Valve Replacement with TiO_2 Nanocrystalline Film Material

Xiong Tan[#], Jinjie Li[#], Weitao Jin, Bo Mei, Guangjie He, Yali Wang, Shuliang Wei, Yinglong Lai[*]

Department of Cardiothoracic Surgery, Affiliated Hospital of North Sichuan Medical College, Nanchong, 637000, China

#These authors contributed equally to this work

ARTICLE INFO

Original paper

Article history:
Received: December 04, 2021
Accepted: March 07, 2022
Published: March 31, 2022

Keywords:
TiO_2 nanocrystalline film, heart valve replacement, cardiac self-recovery, aortic root, papaverine infusion

ABSTRACT

This work was to investigate TiO_2 nanocrystalline film material in heart valve replacement (HVR) and the effect of papaverine infusion through the aortic root before cardiac self-recovery during the HVR. TiO_2 nanocrystalline films were prepared by radio frequency (RF) reactive sputtering. The crystallization characteristics and surface morphology of TiO_2 nanocrystalline films were observed by X-ray diffraction and scanning electron microscopy, and the anti-platelet adhesion and anti-coagulation properties of the films were analyzed. 86 patients with heart valve disease were selected and all underwent HVR. They were randomly divided into a control group (routine treatment) and an experimental group (papaverine perfusion through aortic root), with 43 cases in each group. The rate of cardiac self-recovery and the dosage of dopamine were observed. The results showed that the TiO_2 nanocrystalline film was composed of a large number of uniform particles, and the average particle size was about 18.97 ± 7.28 nm. The rate of cardiac self-recovery in the experimental group was 97.67%, which was significantly higher than that in the control group (67.44%) ($P< 0.05$). The dosage of epinephrine, dopamine, and duration of cardiopulmonary bypass (CPB) assistance in the observation group were less than those in the control group ($P < 0.05$). These results indicated that TiO_2 nanocrystalline film could be used in HVR, and papaverine infusion through aortic root before HVR and myocardial protection measures can significantly improve the rate of cardiac self-recovery and promote postoperative recovery.

DOI: http://dx.doi.org/10.14715/cmb/2022.68.3.35

Introduction

Heart valve replacement (HVR) requires temporary cutting off of cardiac coronary circulation. Although cardiac arrest fluid and low temperature can be used to protect the heart, the metabolism of cardiac cells is not completely stopped during aortic dissection, resulting in changes in the structure and function of cardiac cells (1-3). Cardiopulmonary bypass (CPB) can ensure the blood perfusion and oxygen supply to the patient's organs, so as to maintain the dynamic balance of the internal environment and protect the vital organ function from damage (4-6). However, CPB can lead to systemic inflammatory response syndrome, elevate the level of myocardial injury, and increase the incidence of postoperative complications. Moreover, myocardial ischemia/reperfusion injury after occlusion is also a key factor leading to myocardial injury (7). Papaverine has a direct and non-specific relaxation effect on blood vessels, heart or other smooth muscles, and is widely used in the treatment of ischemia caused by the cardiac, brain, and peripheral vascular spasm (8-10).

TiO_2 Nanocrystalline film material has been widely used as surface modification material for vascular medical devices (such as artificial vascular stents and artificial heart valves) due to its excellent anticoagulant properties and endothelial cell growth guidance (11-13). Líšková et al. (2020) (14) pointed out that the excellent anticoagulant energy of TiO_2 Nanocrystalline film material has exceeded that of pyrolytic carbon material with the highest anticoagulant level. Only after systematic biological evaluation and all compliance with national standards can surface-modified medical device materials enter clinical application (15-17). Therefore, the detection of TiO_2 Nanocrystalline film material can provide an experimental and theoretical basis for the application of TiO_2 Nanocrystalline film in the surface modification of vascular implant devices.

From January 2019 to December 2021, 86 patients

*Corresponding author. E-mail: daiyubi41032251@163.com

with heart valve disease who underwent HVR were selected and were randomly divided into a control group and an experimental group. In the experimental group, 43 patients received papaverine perfusion through the aortic root to protect the myocardium before cardiac self-recovery during CPB and finally achieved a good therapeutic effect. The objective of this work was to improve the intraoperative rate of cardiac self-recovery and reduce the CPB auxiliary time to improve the myocardial protection effect and postoperative improvement.

Materials and methods

Research objects

In this work, 86 patients with heart valve disease treated in our hospital from January 2019 to December 2021 were selected as the research objects, and all underwent HVR. They were divided into a control group (routine treatment) and an experimental group (papaverine perfusion through aortic root) by random number table method, with 43 cases in each group. There were 47 males and 39 females, with an average age of 43.4 ± 11.5 years old. There was no significant difference in basic information between the two groups (P> 0.05). This work was approved by the Medical Ethics Committee of Affiliated Hospital of North Sichuan Medical College. Patients and their families were informed of the experiment and signed informed consent.

Inclusion criteria were given as follows: patients with heart valve disease diagnosed according to clinical symptoms, manifestation signs, and color echocardiography; and patients with HVR surgery indications.

Exclusion criteria were set as follows: patients combined with angina pectoris and myocardial ischemia, or coronary heart disease confirmed by preoperative coronary angiography; patients with infective endocarditis; patients with recurrent heart valve surgery; and patients with liver, kidney, spleen, and other organs failure.

Surgery methods

All patients received endotracheal intubation, intravenous combined general anesthesia, and underwent surgery under conventional CPB and open heart vision. CPB was constructed by the conventional method through the median sternal incision, followed by parallel circulation after heparinization. The ascending aorta was blocked and cardiac arrest fluid was injected into the aortic root. The temperature was 30 ~ 32℃ during the surgery. The mitral and aortic valves were double-bladed mechanical valves (including TiO2 Nanocrystalline film), the tricuspid valve was formed using BalMedic soft ring (Beijing Bailensee Bioengineering Co., LTD., China), and the Atricure bipolar radio frequency (RF) pen was used.

In the control group, aorta blocking forceps were opened after full exhaust, cardioplegia fluid was routinely poured, and defibrillation was performed when necessary.

After ascending aorta occlusion, the experimental group was infused with hemostasis fluid. When the heart did not beat effectively, papaverine (60 mg diluted to 20 mL) was injected through the aortic root perfusion tube, and repeated aspirations were performed 8 to 10 times, with a cumulative total of 140 to 210 mL, followed by continuous infusion of arrest fluid. When the heart showed signs of spontaneous beating, the aortic blocking forceps were opened and the aortic root was pressed with high frequency by hand to ensure that the aorta was completely closed each time.

Observation indicators

The aortic occlusion time (min), rate of cardiac self-recovery (%), duration of CPB assistance after cardiac self-recovery (min), amount of dopamine (μg/ (kg·min)), amount of adrenaline (μg/ (kg·min)), duration of ventilator assisted breathing (min), perioperative complications, and length of hospital stay (d) and patients in two groups were recorded and compared. In addition, a 1-year follow-up was performed.

Preparation of TiO_2 nanocrystalline film

TiO_2 Nanocrystalline film was prepared by RF reactive sputtering. TiO_2 Nanocrystalline film was prepared on a BMS500B RF sputtering machine (Chengdu Sideng Technology Co., LTD.) equipped with 1 DC sputtering target and 2 RF sputtering targets. The experimental target was TiO2 with 99.99 % purity, and the sputtering gas was argon. RF sputtering power was 200 W, and frequency was 13.56 MHz. The limit vacuum of the vacuum chamber was pumped to 1 $\times 10^{-4}$ Pa, and the sputtering pressure

was 0.5 ~ 2 Pa. Clean ordinary slides were used for substrate without heating, and the deposition time of TiO2 Nanocrystalline film was 2 h. TiO_2 Nanocrystalline film samples were annealed at 200°C, 300℃, 400℃, and 500℃ for 1 h, respectively.

Characterization of TiO_2 nanocrystalline film

The crystal structure of the electrode material was observed by X-ray diffraction (XRD, PW1710 X-ray Diffractometer, Philips, Netherlands) with a CuK α source of 30 kV, 20 mA, and a wavelength of 0.15418 nm. The Scherrer formula was used to estimate the diffraction peak and calculate the grain size of the film, as shown in equation (1). The morphology was characterized by Nova Nano SEM ×30 field emission scanning electron microscope (SEM, FEI Company of America). SPA400 atomic microscope (AFM, Seiko Co., LTD., Japan) was adopted for scanning imaging of thin-film samples in contact mode, scanning range of 1 μm × 1 μm. The grain size was analyzed and characterized by a TU-1901 UV-vis spectrophotometer (TU-1901, Beijing General Analysis Co., LTD.). The transmission spectra of the films were measured by a TU-1901 UV-vis spectrophotometer in the range of 200 ~ 1050 nm.

$$S = \frac{k\lambda}{w \times \beta} \quad [1]$$

In the above equation, S represented the grain size, k represented the constant and k = 0.89, w referred to the half-width of the X-ray diffraction peak, and β represented the Bragg Angle.

Determination of the anticoagulant activity of film

The prepared TiO_2 Nanocrystalline film was ultrasonic washed with acetone, ethanol and deionized water for 5min in turn, and then dried for backup use. 10 mL venous blood of healthy adults was extracted with a plastic syringe, and 0.03 mL blood was dropped on the surface of the film. Then, the film was immersed in 30 mL distilled water after standing for 10 min ~ 40 min, standing for 10min each time. When the unsolidified red blood cells were fully dissolved in water, 722 visible light spectrophotometer (Shanghai Kexiao Scientific Instrument Co., LTD.) was used to measure the red blood cell photometric value in water and obtain the data on dynamic blood loss time. The film samples were placed in platelet-rich plasma and incubated in a 37°C water bath at constant temperature for 1 h. After removal, the test tube was placed in 0.9% NaCl to clean the non-adherent platelets and fixed in 3 - 5% glutaraldehyde solution for 3 h. Gradient alcohol was used for dehydration, and gradient iso-pentacyl acetate was dealcoholized. After a thin layer of gold, the powder was sprayed on the surface, the SEM was used to qualitatively analyze the morphological changes of platelets and t-film morphology.

Statistical methods

All the data in this work were established in an Excel database and analyzed by SPSS20.0. The measurement data were expressed as mean ± standard deviation ($\bar{x} \pm s$), the counting data were expressed by χ^2 test, and the counting data were expressed as a percentage (%). The difference was statistically significant at $P < 0.05$.

Results and discussion

Characterization of surface morphology of thin films

Since TiO_2 Nanocrystalline film was an insulating film, a very thin layer of gold powder should be sprayed on its surface before SEM observation. By observing the SEM images of TiO_2 Nanocrystalline film, it was found that TiO_2 Nanocrystalline film was composed of a large number of homogeneous particles with an average particle size of 18.97 ± 7.28 nm. The illustration in Figure 1B was a cross-section photo of TiO_2 Nanocrystalline film. The section photo in Figure 1B showed that the thickness of TiO_2 Nanocrystalline film was about 5.24 nm. Atomic force microscopy (AFM) was shown in Figure 2. It was found that the film surface was relatively smooth, and the sample surface roughness was 6.43 nm.

Crystal structure of the film

TiO_2 Nanocrystalline film was prepared by RF reactive sputtering with P25 as raw material. XRD was used to analyze TiO_2 Nanocrystalline film prepared at room temperature after annealing at 200-500°C for 1 h. The results were shown in Figure 3, which illustrated that TiO_2 Nanocrystalline film prepared at room temperature showed an amorphous structure. After annealing at 200℃ and 300℃ for 1 h, the crystal morphology did not change, and after

annealing at 400℃, the crystal morphology changed. The diffraction peaks at 2θ were 25.6°, 37.8°, 56.6°, and 67.7°, which correspond to the characteristic diffraction peaks of the crystal planes of anatase TiO^2 (101), (200), (211), and (204), respectively. In addition, the characteristic diffraction peaks of rutile TiO^2 appeared at diffraction angles of 28.7°, 46.3°, 57.2°, and 64.7°. When the annealing temperature rose to 500℃, the intensity of the peak increased.

Optical properties of films

Tu-1901 UV-visible spectrophotometer was used to test the average transmittance of TiO_2 Nanocrystalline film annealed at different sputtering pressures. The test results were shown in Figure 4. The average transmittance of TiO_2 Nanocrystalline film was more than 85% in the range of 400 ~ 900 nm.

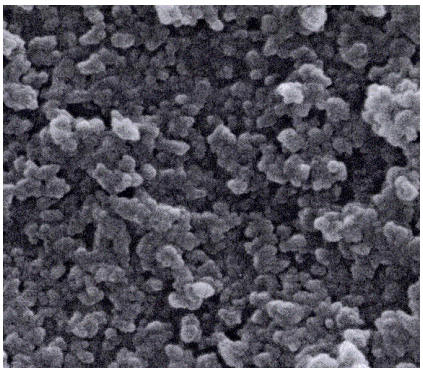

Figure 1. SEM images of TiO_2 nanocrystalline film. (A): SEM image of TiO2 nanocrystalline film; (B): Section photo of TiO_2 nanocrystalline film

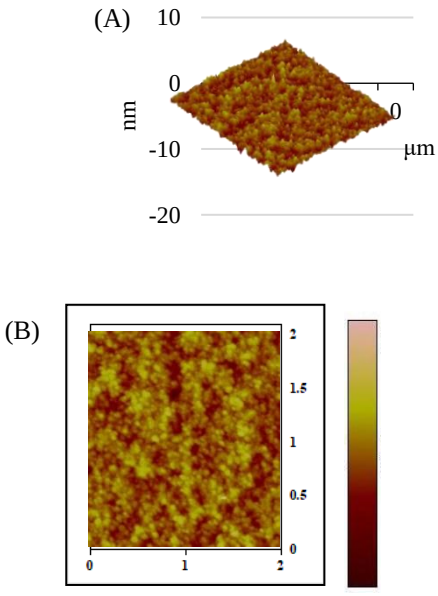

Figure 2. AFM images. (A): 2Dimage; (B): 3D image

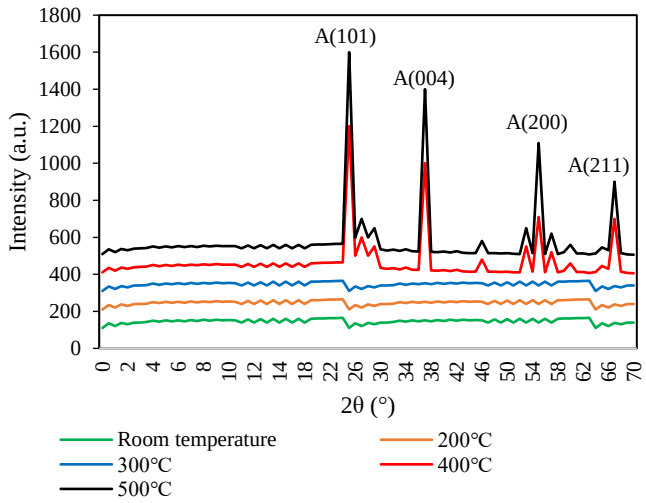

Figure 3. XRD pattern of TiO2 Nanocrystalline film at different annealing temperatures (1 h).

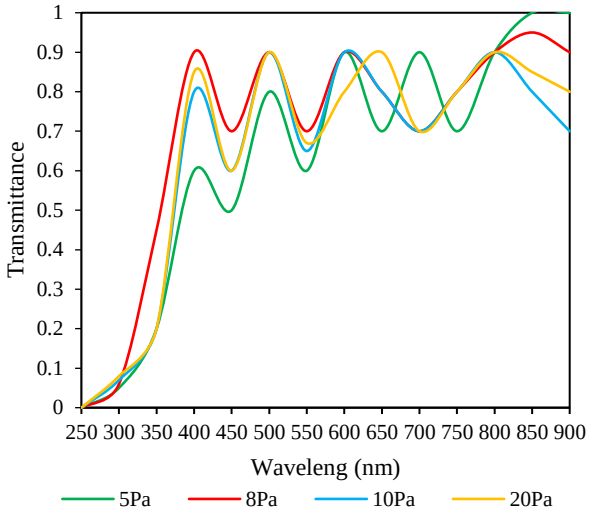

Figure 4. Transmission spectra of TiO_2 films prepared at different sputtering pressures.

Platelet adhesion and anticoagulant activity

The more platelets adhere to the material, the more serious the deformation will be, and the more activated the number, indicating that the material and blood compatibility was worse; otherwise, the compatibility was better. As shown in Figure 5, the three materials were ranked from high to low according to the number of platelet adhesion on the surface and the degree of deformation: industrial pure titanium, nanocrystalline titanium, and TiO_2 Nanocrystalline film in order.

Because the surface properties of different materials were different, the degree of contact with blood coagulation was not the same. According to Figure 6, several materials can be sorted from long to

short in terms of coagulation time as follows: TiO_2 Nanocrystalline film, nanocrystal titanium, and industrial pure titanium. It indicated that the anticoagulant activity of TiO_2 Nanocrystalline film can be significantly improved.

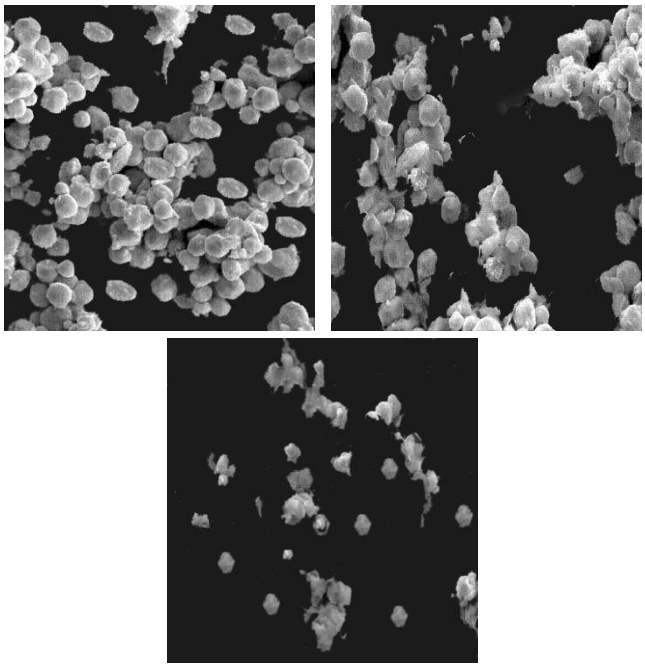

Figure 5. Electron microscopy of platelet adhesion of different materials. (A): industrial pure titanium; (B): nanocrystal titanium; and (C): TiO_2 nanocrystalline film

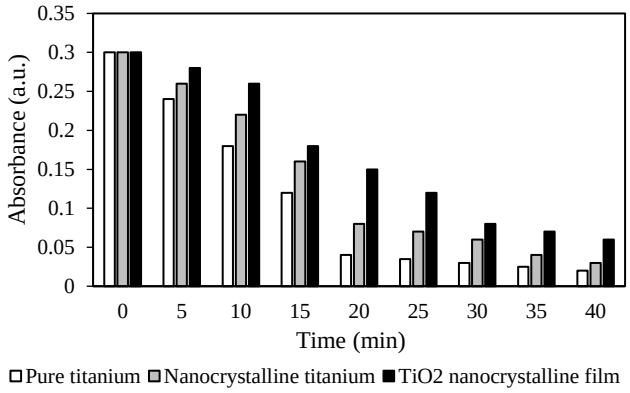

Figure 6. Histogram of dynamic coagulation time of different materials.

Comparison of general data of patients in two groups

There were no statistically significant differences in gender, age, body weight, preoperative cardiac function level, left ventricular ejection fraction (LVEF), disease type, and surgical methods between the two groups, as shown in Table 1.

Table 1. Comparison on general data of patients (n, $\bar{x} \pm s$)

Indicator	Control group (n = 43)	Experimental group (n = 43)	*P*
Gender			
Males	25	22	> 0.05
Females	18	21	
Age (years old)	42.35 ± 11.48	43.37 ± 10.42	> 0.05
Body weight (kg)	56.72 ± 9.72	54.46 ± 8.71	> 0.05
Cardiac function level			> 0.05
Level II	27	29	
Level III	16	14	
LVEF (%)	61.67 ± 6.78	61.58 ± 7.23	> 0.05
Disease type			> 0.05
Mitral stenosis	18	15	
Mitral insufficiency	7	8	
Aortic insufficiency	8	9	
Tricuspid stenosis	10	11	
Surgery method			> 0.05
Mitral valve replacement	16	19	
Aortic valve replacement	13	12	
Double valve replacement	9	8	
Tricuspid valve plasty	5	4	

Comparison of clinical results between the two groups

The duration of CPB assistance, the amount of dopamine, and the amount of epinephrine used in the experimental group after the cardiac self-recovery during the surgery were shorter or less than those in the control group. The rate of cardiac self-recovery (97.67%) was higher than that of the control group (67.44%), with statistical significance ($P< 0.05$). There were no significant differences in aortic occlusion time, duration of ventilator-assisted breathing, and hospital stay between the control group and the control group ($P> 0.05$), as shown in Table 2.

Table 2. Comparison of clinical results between the two groups (n, $\bar{x} \pm s$)

Indicator	Control group (n = 43)	Experimental group (n = 43)	t/χ^2	*P*
Aortic occlusion time (min)	45.62 ± 10.45	46.78 ± 9.85	1.873	P > 0.05
Rate of cardiac self-recovery (%)	67.44	97.67*	-0.653	P < 0.05
Duration of CPB assistance after cardiac self-recovery (min)	24.54 ± 11.43	12.56 ± 9.67	-1.241	P < 0.05
Dopamine (μg/ (kg·min))	6.57 ± 2.71	3.27 ± 1.73	-0.973	P < 0.05
Adrenaline (μg/ (kg·min))	0.064 ± 0.018	0.021 ± 0.013	-0.765	P < 0.05
Duration of ventilator assisted breathing (h)	10.26 ± 4.25	10.21 ± 4.76	1.542	P > 0.05
Hospital stay (d)	7.78 ± 2.18	7.51 ± 2.15	1.525	P > 0.05

Comparison of complications between the two groups

There was no death in either group. The experimental group followed up 43 cases for 6 - 12

months. During the follow-up period, 6 patients were readmitted due to cardiac events, including 1 case of myocardial infarction, 1 case of severe angina pectoris, 2 cases of cerebral infarction, and 2 cases of gastrointestinal bleeding. In the control group, 43 patients were followed up for 7 - 12 months. During the follow-up period, 8 patients were readmitted to the hospital due to cardiac events, including 1 case of myocardial infarction, 3 cases of severe angina pectoris, 3 cases of cerebral infarction, and 1 case of gastrointestinal bleeding. The complications in the 1-year follow-up were shown in Table 3.

Table 3. Complications in 1-year follow-up after surgery (n)

Item	Control group (n = 43)	Experimental group (n = 43)	t/χ^2	*P*
Myocardial infarction	1	1	0.556	P > 0.05
Severe angina pectoris	3	1	-0.783	P < 0.05
Cerebral infarction	3	2	0.672	P > 0.05
Gastrointestinal hemorrhage	1	2	0.874	P > 0.05
Death	0	0		P > 0.05

With the continuous improvement of cardiac surgery and CPB application technology, the effectiveness and safety of open-heart surgery in the treatment of heart valve disease have been guaranteed. However, postoperative myocardial injury is still a risk factor for complications after CPB open heart surgery, and excellent myocardial protection directly affects the success or failure of cardiac surgery and patient prognosis (18-20). In this work, papaverine was used to improve the rate of cardiac self-recovery. Papaverine can improve the intraoperative blood oxygen supply of the myocardium and improve the internal environment of ischemia and hypoxia (21).

In this work, TiO_2 Nanocrystalline film was successfully prepared by RF reactive sputtering. The crystal characteristics and surface morphology of TiO_2 Nanocrystalline film were observed by X-ray diffraction and scanning electron microscopy, and the antiplatelet adhesion and anticoagulant properties of the film were analyzed. It was observed by electron microscope that the prepared TiO_2 nanocrystalline film was composed of a large number of homogeneous particles with an average particle size of 18.97 ± 7.28 nm. In addition, TiO_2 Nanocrystalline film was found to have good anti-platelet adhesion and anti-whole blood coagulation properties (22-24). In this work, TiO_2 Nanocrystalline film was applied to HVR. After ascending aorta occlusion, patients in the experimental group were injected with blood-containing cardiac arrest fluid. When the heart did not beat effectively, papaverine was injected through aortic root perfusion tube (diluted 60 mg to 20 mL), which can make Papaverine directly enter the coronary artery. When the coronary arteries were dilated to the maximum extent, adequate perfusion of arrest fluid can be ensured to achieve myocardial protection. In the hypothermia state, coronary arteries are generally in a spasm state. Although the anastomosis of target vessels can be accurately found in the concurrent CPB process, it is a technical difficulty in clinical operation practice. In this work, papaverine can continuously dilate coronary arteries and provide basic conditions for the heart to accurately find coronary arteries when it stopped beating (25-27). Good myocardial protection measures can shorten the duration of CPB assistance and reduce the use of positive inotropic drugs such as dopamine and norepinephrine. Ray et al. (2017) (28) also achieved good clinical treatment effect by using poppy perfusion to the aortic root before cardiac valve surgery, which was consistent with the results of this work.

Some points should also be noted in the clinical practice of Papaverine. Firstly, during repeated aspiration, a little blood should be left in the syringe after each infusion of blood into the aorta, otherwise, some air will directly enter the coronary artery. Secondly, when squeezing the ascending aorta, the plaque should be avoided as far as possible.

There were some shortcomings in this work. Only one preparation method was used in the preparation of TiO_2 Nanocrystalline film. A variety of preparation methods should be used to compare TiO_2 Nanocrystalline film with different grain sizes. In the later stage, the processing process should be optimized to prepare films with different grain sizes and good morphology.

Conclusions

TiO_2 Nanocrystalline film was prepared by RF reactive sputtering. HVR was performed in 86 patients with heart valve diseases. In the experimental group, papaverine was injected into the aortic root to protect the myocardium before cardiac self-recovery during CPB, aiming to improve the intraoperative rate of

cardiac self-recovery and reduce the duration of CPB assistance and enhance the effect of myocardial protection. The results showed that TiO_2 Nanocrystalline film could be used for HVR. Papaverine infusion and myocardial protection before HVR can significantly improve the rate of cardiac self-recovery and promote postoperative recovery. The limitation of this work was that the preparation process was single and the sample size was small. In the later stage, the preparation process should be optimized and the sample size should be increased to further explore and verify the conclusions. In conclusion, this work provided an experimental and theoretical basis for the surface modification application of vascular implant devices, and on the other hand, it also enriched the research content of biological safety of nanomaterials.

Acknowledgments

Not applicable.

Interest conflict

The authors declare that they have no conflict of interest.

References

1. Surabhi S, Kumar M. Comparison of ringer's lactate and plasmalyt-a as cardiopulmonary bypass prime for bypass associated acidosis in valve replacement surgeries. Ann Card Anaesth. 2021 Jan-Mar;24(1):36-41. doi: 10.4103/aca.ACA_104_19. PMID: 33938829; PMCID: PMC8081150.
2. Politi MT, Ochoa F, Netti V, Ferreyra R, Bortman G, Sanjuan N, Morales C, Piazza A, Capurro C. Changes in cardiac Aquaporin expression during aortic valve replacement surgery with cardiopulmonary bypass. Eur J Cardiothorac Surg. 2020 Mar 1;57(3):556-564. doi: 10.1093/ejcts/ezz249. PMID: 31535145.
3. Lee JH, Lee JE, Shin J, Song IK, Kim HS, Kim CS, Kim WH, Kim JT. Clinical implications of hypothermic ventricular fibrillation versus beating-heart technique during cardiopulmonary bypass for pulmonary valve replacement in patients with repaired tetralogy of Fallot. Interact Cardiovasc Thorac Surg. 2017 Sep 1;25(3):370-376. doi: 10.1093/icvts/ivx148. PMID: 28535202.
4. Luo Z, Wei X, Zuo Y, Du G. Sevoflurane- and propofol-based regimens show comparable effect on oxygenation in patients undergoing cardiac valve replacement with cardiopulmonary bypass. Cardiovasc J Afr. 2020 Mar/Apr;31(4):71-74. doi: 10.5830/CVJA-2019-050. Epub 2019 Sep 11. PMID: 31512716.
5. Song J, Yao L, Zhao L, Du B, Liu L, Chen J. Changes in the concentrations of mediators in exhaled breath condensate during cardiac valve replacement under cardiopulmonary bypass and their relations with postoperative acute respiratory distress syndrome. Medicine (Baltimore). 2020 May 22;99(21):e20007. doi: 10.1097/MD.0000000000020007. PMID: 32481266; PMCID: PMC7249883.
6. Zhu J, Zhang W, Shen G, Yu X, Guo J, Zhong T. Lund exhaust on hemodynamic parameters and inflammatory mediators in patients undergoing cardiac valve replacement under cardiopulmonary bypass. Exp Ther Med. 2018 Sep;16(3):1747-1752. doi: 10.3892/etm.2018.6354. Epub 2018 Jun 26. PMID: 30186397; PMCID: PMC6122371.
7. Yamamoto T, Endo D, Yamaoka H, Shimada A, Matsushita S, Amano A. Rapid-Deployment Aortic Valve Replacement for a Hemodialysis Patient with Prior Coronary Artery Bypass Grafting. Heart Surg Forum. 2021 Jun 11;24(3):E530-E533. doi: 10.1532/hsf.3535. PMID: 34173768.
8. Li W, Jiao C, Lai D, Wu D, You Z, Feng L, Wu X, Zhang J. Papaverine Perfusion via the Aortic Root before Heart Re-beating Alleviates Myocardial Injury after Heart Valve Replacement. Arch Med Res. 2021 May;52(4):405-413. doi: 10.1016/j.arcmed.2020.12.006. Epub 2021 Jan 15. PMID: 33461822.
9. Duan T, Zhang J, Xiang D, Song R, Kong R, Xu D. Effectiveness and safety of intracoronary papaverine, alprostadil, and high dosages of nicorandil and adenosine triphosphate for measurement of the index of coronary microcirculatory resistance in a pig model. Adv Clin Exp Med. 2019 Oct;28(10):1409-1418. doi: 10.17219/acem/104541. PMID: 31638745.
10. Nauchi M, Sakai T, Yamawaki M, Ito Y. Sinus Standstill in a Patient after Intracoronary Papaverine Administration for a Coronary Fractional Flow Reserve. Int Heart J. 2018 May 30;59(3):630-633. doi: 10.1536/ihj.17-294. Epub 2018 May 20. PMID: 29681575.
11. Wei M, Peng XL, Liu QS, Li F, Yao MM. Nanocrystalline TiO_2 Composite Films for the Photodegradation of Formaldehyde and Oxytetracycline under Visible Light Irradiation. Molecules. 2017 Jun 14;22(6):950. doi: 10.3390/molecules22060950. PMID: 28613235; PMCID: PMC6152682.
12. Zukalová M, Vinarčíková M, Bouša M, Kavan L. Nanocrystalline TiO2/Carbon/Sulfur Composite Cathodes for Lithium-Sulfur Battery. Nanomaterials (Basel). 2021 Feb 20;11(2):541. doi: 10.3390/nano11020541. PMID: 33672643; PMCID: PMC7924192.
13. Hu K, Sampaio RN, Schneider J, Troian-Gautier L, Meyer GJ. Perspectives on Dye Sensitization of Nanocrystalline Mesoporous Thin Films. J Am Chem Soc. 2020 Sep 23;142(38):16099-16116. doi: 10.1021/jacs.0c04886. Epub 2020 Sep 3. PMID: 32818372.

14. Líšková A, Letašiová S, Jantová S, Brezová V, Kandarova H. Evaluation of phototoxic and cytotoxic potential of TiO2 nanosheets in a 3D reconstructed human skin model. ALTEX. 2020;37(3):441-450. doi: 10.14573/altex.1910012. Epub 2020 Feb 25. PMID: 32113185.
15. Bruzzi M, Mori R, Baldi A, Carnevale EA, Cavallaro A, Scaringella M. Thermally Stimulated Currents in Nanocrystalline Titania. Nanomaterials (Basel). 2018 Jan 5;8(1):13. doi: 10.3390/nano8010013. PMID: 29303976; PMCID: PMC5791100.
16. Hellner B, Stegmann AE, Pushpavanam K, Bailey MJ, Baneyx F. Phase Control of Nanocrystalline Inclusions in Bioprecipitated Titania with a Panel of Mutant Silica-Binding Proteins. Langmuir. 2020 Jul 28;36(29):8503-8510. doi: 10.1021/acs.langmuir.0c01108. Epub 2020 Jul 16. PMID: 32614593.
17. RanguMagar AB, Chhetri BP, Parameswaran-Thankam A, Watanabe F, Sinha A, Kim JW, Saini V, Biris AS, Ghosh A. Nanocrystalline Cellulose-Derived Doped Carbonaceous Material for Rapid Mineralization of Nitrophenols under Visible Light. ACS Omega. 2018 Jul 19;3(7):8111-8121. doi: 10.1021/acsomega.8b01020. PMID: 31458947; PMCID: PMC6644635.
18. Cammertoni F, Bruno P, Pavone N, Farina P, Mazza A, Iafrancesco M, Nesta M, Chiariello GA, Spalletta C, Cavaliere F, Calabrese M, D'Angelo GA, Sanesi V, Conti F, D'Errico D, Massetti M. Influence of cardiopulmonary bypass set-up and management on clinical outcomes after minimally invasive aortic valve surgery. Perfusion. 2021 Oct;36(7):679-687. doi: 10.1177/02676591211023301. Epub 2021 Jun 3. PMID: 34080484.
19. Spiliopoulos K, Schmid FX. A technique to resect the Edwards SAPIEN 3 Transcatheter Heart Valve 18 months after implantation in case of surgical aortic valve replacement. Gen Thorac Cardiovasc Surg. 2021 Apr;69(4):774-777. doi: 10.1007/s11748-020-01529-6. Epub 2020 Oct 27. PMID: 33108610.
20. Zhou H, Zhou D, Lu J, Wu C, Zhu Z. Effects of Pre-Cardiopulmonary Bypass Administration of Dexmedetomidine on Cardiac Injuries and the Inflammatory Response in Valve Replacement Surgery with a Sevoflurane Postconditioning Protocol: A Pilot Study. J Cardiovasc Pharmacol. 2019 Aug;74(2):91-97. doi: 10.1097/FJC.0000000000000698. PMID: 31356535; PMCID: PMC6688713.
21. Hernández JJ, Ragone MI, Bonazzola P, Bandoni AL, Consolini AE. Antitussive, antispasmodic, bronchodilating and cardiac inotropic effects of the essential oil from Blepharocalyx salicifolius leaves. J Ethnopharmacol. 2018 Jan 10;210:107-117. doi: 10.1016/j.jep.2017.08.013. Epub 2017 Aug 12. PMID: 28811222.
22. Gonçalves MC, Pereira JC, Matos JC, Vasconcelos HC. Photonic Band Gap and Bactericide Performance of Amorphous Sol-Gel Titania: An Alternative to Crystalline TiO_2. Molecules. 2018 Jul 10;23(7):1677. doi: 10.3390/molecules23071677. PMID: 29996500; PMCID: PMC6100469.
23. Šťastný M, Štengl V, Štenglová-Netíková I, Šrámová-Slušná M, Janoš P. Removal of anthracycline cytostatics from aquatic environment: Comparison of nanocrystalline titanium dioxide and decontamination agents. PLoS One. 2019 Oct 11;14(10):e0223117. doi: 10.1371/journal.pone.0223117. PMID: 31603899; PMCID: PMC6788709.
24. Shchelokov A, Palko N, Potemkin V, Grishina M, Morozov R, Korina E, Uchaev D, Krivtsov I, Bol'shakov O. Adsorption of Native Amino Acids on Nanocrystalline TiO2: Physical Chemistry, QSPR, and Theoretical Modeling. Langmuir. 2019 Jan 15;35(2):538-550. doi: 10.1021/acs.langmuir.8b02007. Epub 2018 Dec 28. PMID: 30554513.
25. Kawase Y, Omori H, Kawasaki M, Tanigaki T, Hirata T, Okamoto S, Ota H, Kikuchi J, Okubo M, Kamiya H, Hirakawa A, Suzuki T, Matsuo H. Postocclusional Hyperemia for Fractional Flow Reserve After Percutaneous Coronary Intervention. Circ Cardiovasc Interv. 2017 Dec;10(12):e005674. doi: 10.1161/CIRCINTERVENTIONS.117.005674. PMID: 29246913.
26. Armstead WM, Vavilala MS. Cerebral Perfusion Pressure Directed-Therapy Modulates Cardiac Dysfunction After Traumatic Brain Injury to Influence Cerebral Autoregulation in Pigs. Neurocrit Care. 2019 Dec;31(3):476-485. doi: 10.1007/s12028-019-00735-2. PMID: 31115824; PMCID: PMC6868312.
27. Ruzsa Z, Róna S, Tóth GG, Sótonyi P, Bertrand OF, Nemes B, Merkely B, Hüttl K. Fractional flow reserve in below the knee arteries with critical limb ischemia and validation against gold-standard morphologic, functional measures and long term clinical outcomes. Cardiovasc Revasc Med. 2018 Mar;19(2):175-181. doi: 10.1016/j.carrev.2017.07.007. Epub 2017 Jul 18. PMID: 28866449.
28. Ray Mohapatra CK, Mishra P, Saxena P, Raut C, Khandekar J, Ammannaya GK, Seth HS, Shah V, Singh J. Use of nitroglycerin and verapamil solution by organ bath technique in preparation of left internal thoracic artery for coronary artery bypass surgery. Indian Heart J. 2017 Nov-Dec;69(6):772-776. doi: 10.1016/j.ihj.2017.04.004. Epub 2017 Apr 14. PMID: 29174257; PMCID: PMC5717283.